Planetary and Space Science 59 (2011) 1384–1392

Contents lists available at ScienceDirect

Planetary and Space Science

journal homepage: www.elsevier.com/locate/pss

Landslides in Valles Marineris (Mars): A possible role of basal lubrication by sub-surface ice

Fabio Vittorio De Blasio *

NHAZCA S.r.l., spin-off "Sapienza Università di Roma", Via Cori snc 00177, Italy

ARTICLE INFO

Article history:
Received 19 October 2010
Received in revised form
26 April 2011
Accepted 27 April 2011
Available online 20 May 2011

Keywords:
Mars
Valles Marineris
Landslides
Ice
Evaporites
Mars climate

ABSTRACT

There is much interest on the occurrence of water and ice in the past history of Mars. Because landslides on Mars are much better conserved than their terrestrial counterparts, a physical examination and morphological analysis can reveal significant details on the depositional environment at the instant of failure. A study of the landslides in Valles Marineris based on their physical aspect is presented and the velocity of the landslides is calculated with a stretching block model. The results show that the landslides were subject to strong basal lubrication that made them travel at high speed and to long distances. We use physical analysis to explore the four alternative possibilities that the natural lubricant of the landslides in Valles Marineris was either ice, deep water, a shallow carpet of water, or evaporites. Examination of the furrows present on the surface of the landslide deposits shows that either sub-surface ice or evaporites were likely present on the floor of Valles Marineris during the mass failures.

1. Introduction

In the last decades, the exploration of Mars has revealed numerous novel details of the planet's surface (Carr, 2006), demonstrating that the climate has been warmer and wetter than the present one. Whereas dendritic river networks, gigantic outflow channels, and traces of lakes and deep water basins show the importance of running water and ice in shaping some surface features of Noachian and Hesperian Mars, remnants of glaciers and glacial activity demonstrate the episodic presence of an icy surface also in more recent times (e.g., Kargel, 2004). This paper explores further the possibility that a physical–morphological analysis of Martian landslide deposits offers to increase our understanding of the past climate of Mars. Because on our planet the vigorous geological activity coupled to biological action and robust weathering rapidly erases the traces of landslides, the morphological details of ancient landslides emerge more clearly on Mars than on Earth. It is well known from studies on Earth that the dynamics of a landslide is sensitive to the conditions of the terrain and to the rheology of the material. For example, mudflows of volcanic origin may become extremely mobile if the water content increases of even a small percentage. Likewise, the spreading of rock avalanches is enhanced by an icy gliding surface or by the presence of a weak layer (see e.g., De Blasio, 2011). As a consequence, the physical–dynamical analysis of landslides on Mars may provide information on the presence of ice, water, or another medium along the slope path, and so give significant contribution to the ongoing discussion of the geology and paleoclimate of the red planet.

The best known Martian landslides punctuate the Chasmata of Valles Marineris, the vast canyon (3500 km long, 300 km wide, and 5–8 km deep) stretching along the equator. Fig. 1A shows a THEMIS image of landslide in Capri Chasma of Valles Marineris, with at least seven landslides appearing in the field. The most evident features of the landslides deposits are the long run-out of the snout (maximum landslide length in the figure is 25 km, even though other landslides in Valles Marineris exhibit even longer run-out length), the tongue-like shape, the tendency to spread on a vast area like a viscous fluid, and the presence of remarkable longitudinal furrows (Fig. 1A and C), appearing also in a limited number of terrestrial landslides (Fig. 1B). Each landslide can be grossly divided into four sub-units (Fig. 2): (1) a collapse zone (A in Fig. 2), where flow structures are not discernible; a chaotic zone (B) with weak furrows along the direction of main flow; a third area (C), where furrows are more apparent; and the final part (D) with curved furrows.

Table 1 gives an estimate of the number of landslide groups exhibiting linear furrows based on visual inspection of THEMIS images. Note that some of the Chasmata such as Ganges Chasma are much richer of furrowed landslides than others. For example, despite its large area Eos Chasma has only one group. Like other Chasmata, Eos Chasma exhibits mass wasting in the form of huge blocky rather than lineated lobes. Altogether, it can be estimated

* Tel.: +4798485472.
E-mail address: fvblasio@geologi.uio.no

0032-0633/$ - see front matter © 2011 Elsevier Ltd. All rights reserved.
doi:10.1016/j.pss.2011.04.015

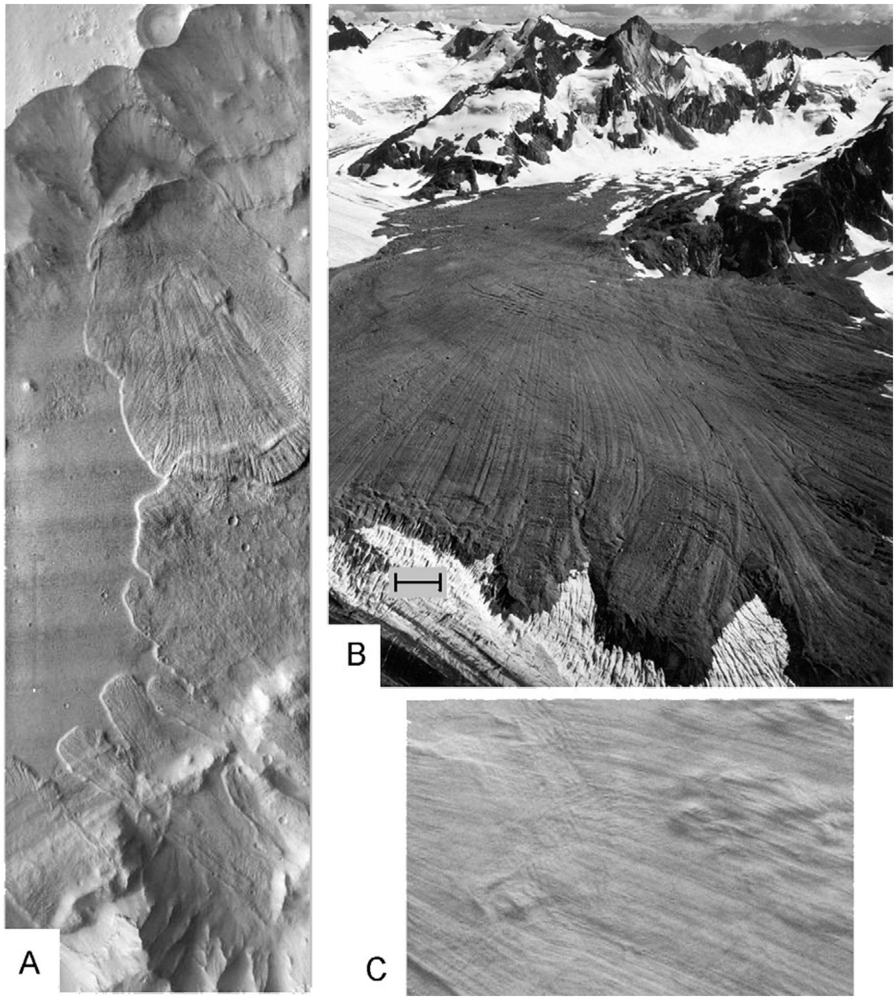

Fig. 1. (A) Valles Marineris hosts among the largest landslides on Mars. Landslides in Capri Chasma. Coordinates: −8.0 N, 318.6 E. Horizontal length 18.4 km. Several landslides are visible in the field. Most of them widened greatly during the flow, while others, visible in the bottom, were more uniform in width. Image Themis V13283001. (B) The Sherman landslide in Alaska. The scale represents 100 m of length. Image courtesy USGS, USA. (C) Detail of a landslide surface in Ganges Chasma. Horizontal length about 11 km. Image Themis PIA20020401, coordinates -8.6 N, 315.7E. (A) and (C) Courtesy NASA/JPL/Space Science Institute.

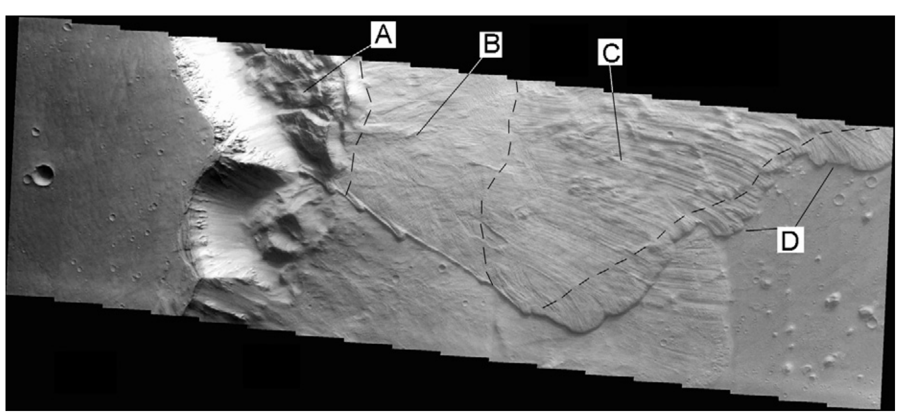

Fig. 2. A couple of landslides in Ganges Chasma. Image Themis PIA09057. Length about 35 km. (A) Chaotic region, (B) flow structures parallel to flow begin to be discernible, (C) furrows become apparent and (D) curved furrows. Courtesy NASA/JPL/Space Science Institute.

that some 10–20% of the landslides in Valles Marineris have evident furrows, even though it is often difficult to discern such structures when more landslides overlap.

The Valles Marineris landslides also exhibit low apparent friction coefficients, defined as the ratio between the vertical fall of the landslide and the horizontal displacement (Scheidegger, 1973). Values range between 0.06 and 0.6 (Lucchitta, 1979), against 0.6–0.9 for rock, thus demonstrating the occurrence of a lubrication effect. A similar tendency of the apparent friction coefficient to decrease for landslides of large volume is exhibited by landslides on Earth (Scheidegger, 1973). A number of explanations have been suggested such as mechanical or acoustic fluidization, thermal effects like vapor or melt lubrication, to name a few (see e.g., Legros, 2002; De Blasio, 2009, 2011 for short

Table 1
Number of landslide groups longer than 10 km and exhibiting furrows on the surface. Two landslides are considered belonging to the same group if they originate from the same scar. A group may so comprise several landslides.

Chasma	Number of groups
Titonium	3
Ius	5
Melas	3
Ophir	4
Coprates	13
Candor	2
Ophir	4
Juventae	0
Ganges	8
Eos	1
Capri	5
Hebes	1

discussions and lists of references). However, although some of the processes invoked for the Earth may be active also for the landslides in Valles Marineris (Harrison and Grimm, 2003), we contend that the dynamics in Valles Marineris is dominated by an effective lubrication at the sole. The main basis for this assertion derives from the morphological analysis of the landslide deposits and in particular from the presence of furrows, as discussed in Section 3. Before such arguments indicating prominence of basal lubrication can be further developed, in Section 2 the velocities of the Valles Marineris mass failure are estimated.

2. Estimates of the velocity based on the observed coefficient of friction

The velocities of Valles Marineris landslides can be computed in the framework of a constant friction model. The friction coefficient can be directly determined as the ratio of the vertical fall to the horizontal travel of the landslide (Scheidegger, 1973). Although crude, a similar analysis reproduces well the observed values of the average velocity for rock avalanches on Earth (e.g., Hsü, 1975; De Blasio, 2011). Calculations are made not only in the hypothesis that the Valles Marineris landslides were subaerial, but also assuming a subaqueous setting. The presence of liquid water on Mars has been suggested either in the form of large reservoirs such as lakes (Lucchitta, 2009) or as an ocean residing in vast regions of the northern lowlands, albeit the ocean was probably not so extensive to reach Valles Marineris (Kargel, 2004; Parker et al., 1993; Carr and Head III, 2003). It has been recently suggested that both the aureoles deposits of Olympus Mons (De Blasio, submitted for publication), and the Valles Marineris mass wasting (Harrison, 2010) might be the product of subaqueous landslides, perhaps deposited in deep lakes occupying the Valles Marineris (Lucchitta, 2009).

Let us start with the case of subaerial failure. Calling x_{CM} the horizontal coordinate of the landslide center of mass, $H(x)$ the height of the terrain at a position x, and μ the friction coefficient, the equation of motion of the center of mass is $dU_{\mathrm{CM}}/dt = g[\sin\beta(x_{\mathrm{CM}}) - \mu\cos\beta(x_{\mathrm{CM}})]$, where $\beta(x)$ is the slope angle in x. The velocity as a function of the position is so $U_{CM}(x_{CM}) = \sqrt{2g[H_0 - H(x_{CM}) - \mu x_{CM}]}$, where H_0 is the initial height of the terrain (at $x=0$) and $g=3.7$ ms^{-2} is the intensity of the gravity field. The friction coefficient follows from the observed run-out of the center of mass R_{CM} imposing $U(R_{CM})=0$, which gives $\mu=(H_0 - H(R_{CM}))/R_{CM}$. Choosing for simplicity the slope path as an exponential function, $H(x) = H_0\exp(-x/L)$, where L gives the length scale of the height decrease, the maximum velocity along the trajectory is found with a simple calculation as $U_{MAX} = \sqrt{2gH_0}\sqrt{1-(\mu L/H_0)(1-\ln(\mu L/H_0))}$. With a set of values $H_0 \approx 4$ km (about half the cliff height in Valles Marineris) and $L=3$ km; $R_{CM}=12$ km consistent with the geometry of slope and landslide travel distance and $\mu=1/3$ compatible with the friction angle from slope stability studies (e.g., Bigot-Cormier and Montgomery, 2007) a high value is found for the maximum velocity reached by the center of mass, $U_{MAX} \approx 109$ ms^{-1}. Even landslides falling from a lower alcove ($H_0 \approx 3$ km) would reach elevated peak velocities, $U_{MAX} \approx 82$ ms^{-1}. Like for other examples on Earth, the landslides in Valles Marineris stretch significantly during flow as a result of fragmentation. This is because a rock avalanche starts as a more or less intact block with cohesion of the order of several MPas (e.g., Schulz, 2002; Bigot-Cormier and Montgomery, 2007) and is fast reduced to a medium of small cohesionless fragments, far more deformable than the original stiff block (Davies and McSaveney, 1999; Locat et al., 2006; Crosta et al., 2007). As a consequence of stretching the front advances more than the center of mass during the same time interval, and thus the velocities of the front will be higher than those of the center of mass.

Velocities for rock avalanches have been measured in a limited number of cases. Often it is the peak or average velocity that is best known (see Sosio et al., 2008 for a recent compilation) while the velocity as a function of time is more difficult to obtain. Recently, the velocity of two landslides triggered by nuclear explosions in Novaya Zemlia test site have been measured with accuracy (Adushkin, 2006). As a simple approximation that proves to be remarkably good for the Novaya Zemlia landslides (De Blasio, 2011), the velocity of the front is calculated as $U_F(x_F) = U_{CM}(x_{CM})[1+\alpha(x_{CM}-x_0)/R_{CM}]$, where $\alpha=(1/2)\Delta L/L_0$ is the total stretching (half the difference between the total landslide length variation ΔL and the landslide length at start L_0). The front velocity, which is also reported in Fig. 3, reaches values far higher than that relative to the center of mass, peaking at nearly $U_{MAX,F} \approx 202$ ms^{-1}. For a gentler terrain, for example with $L=10$ km, the peak velocity of the front is reduced, remaining a still respectable 113 ms^{-1} (in this case the friction coefficient needs to be reduced to 0.23 in order for the landslide center of mass to reach the same distance as the previous case with $L=3$ km). These values of the velocities are high compared to landslides on Earth, which typically fall from lower heights than they do in Valles Marineris.

Note that this failure geometry of a sliding–stretching body is simplified with regard to the actual geometry of a landslide in Valles Marineris. The initial failures typically appear in the form of a "slump" (Schulz, 2002), i.e., a rotational landslide that normally forms in homogeneous terrain. Although the rotational geometry in the failure region may play a role in the initial acceleration, the path of the landslide is dominated by a linear movement along the slope. Thus, the velocities calculated with this simple model should be of the correct order. Note also that in a series of experiments, some amount of granular medium is let to collapse on a horizontal plane,

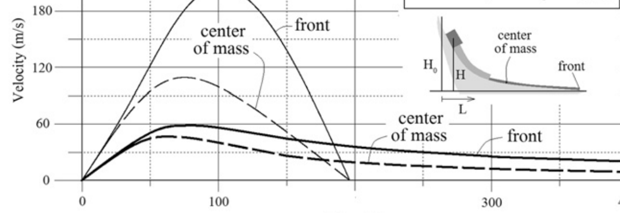

Fig. 3. Calculated landslide velocities for a landslide in Valles Marineris within the framework of a subaerial and a subaqueous model. Data for the subaqueous calculation are $\rho=2700$ kg m^{-3}; $C_D=1.95-0.77(D/W)$; $\alpha=4$; and $C_S=0.003$. The landslide changes its aspect ratio as shown in the inset of the figure, starting as a cube and preserving parallelepiped shape with constant product DL as it stretches along slope.

with an initial geometry of failure resembling the landslides in Valles Marineris (Lajeunesse et al., 2006a). Although providing valuable information, there are also notable differences between the laboratory setting and the landslides in Valles Marineris. Not only are the scale and gravity field very different. It is also not certain whether the material of a slump in Valles Marineris disintegrates at once or remains partly intact for a prolonged time, even though it seems that fragmentation of terrestrial landslides does occur already at the very start of the sliding process (Locat et al., 2006). This makes a significant difference because the experimental failure by Lajeunesse et al. (2006a, b) is driven from the start by the lateral pressure exerted by the granular medium, also called the earth pressure force (e.g., Iverson, 1997), as well as by the vertical push of the falling material. In contrast, the driving force on the intact mass of a slump is due to the gravitational torque, with the earth pressure force playing a role only after strong fragmentation has taken place. In short, the results from small-scale experiments should be applied to large-scale failures with some caution.

If the landslide travels underwater, the resistance due to water drag and buoyancy must be included in the calculations. In addition, the sliding mass must accelerate water, which results in a fictitious increase of the landslide mass, called the added mass (e.g., De Blasio, 2011). In contrast to the subaerial case, where the dimension of the landslide do not influence the dynamics, the dimensions affect the drag force and so the speed as a function of time. Assuming the slide shaped as a parallelepiped of length L, width W and height D (where L and D change with time as the landslide stretches, maintaining the product LD constant), the equation of motion of the front becomes (De Blasio, 2011)

$$\left(1+\alpha\frac{\rho_F}{\rho}\right)\frac{dU}{dt} = \frac{\rho-\rho_F}{\rho} g\sin\beta\left[1-\tan\phi/\tan\beta\right] - \frac{1}{2}\frac{\rho_F}{\rho}\left[\frac{C_D}{L}+\frac{1}{4}\left(\frac{C_S}{D}+2\frac{C_S}{W}\right)\right]U^2, \qquad (1)$$

where ρ and ρ_F are the rock and water densities, respectively, α is the added mass coefficient, $C_D \approx 1-2$ is the pressure drag coefficient (e.g., De Blasio, 2011) and $C_{SF} \approx 0.002-0.006$ is the skin friction coefficient (Schlichting, 1960).

Fig. 3 shows the results of the calculations. While as shown earlier a subaerial landslide preserves a velocity above 100 m/s for most of its path, subaqueous velocities are much reduced, but still high (maximum velocity of the order 200 km/h). In order to reach the observed run-out, the basal friction coefficient in the subaqueous case must be lowered from 1/3 to 0.025, as the use of the same coefficient for the subaqueous case would give too short a runout (lowermost curve in Fig. 3). A possible physical explanation for this reduction is discussed in the next section. Note also that subaqueous landslides take a much longer traveling time than the subaerial ones. Finally, it should be stressed that such calculations are simplified with respect to reality as the geometry, morphometry, and structural characteristics of landslides play an important role in the dynamics (Shea and van Wyk de Vries, 2008).

3. Possible Mechanisms for basal lubrication

Two separate explanations are required for the friction reduction in the subaerial and subaqueous scenarios. In the subaerial case, the lubrication effect should cause a decrease in the friction coefficient by a factor of 2–5 from the value of bare rock. The friction coefficient for the subaqueous case is even smaller (0.025 in the calculation of Fig. 3) because otherwise the drag force exerted by water would make the landslide stop too early.

Let us consider the subaerial case first. The characteristic furrows of the Valles Marineris landslides suggest a comparison with landslides traveling on top of glaciers and in particular with the 1964 Alaskan landslide that fell on the Sherman glacier following a strong earthquake (Shreve, 1966; Sreve, 1968; Marangunic and Bull, 1968; McSaveney, 1978; see also Fig. 1B). The field analysis of Sherman reveals that furrows are V-shaped grooves about 8 m wide and at most 2.5 m deep (Shreve, 1966). Is the resemblance between the ice-lubricated landslide in Sherman and the Valles Marineris landslides a purely external one, or can physical similarities be drawn between the two different environments?

Surprisingly little is known on the physics of landslides traveling on ice. Some numerical calculations (e.g., Sosio et al., 2008) utilize the frictional and the Voellmy models with finite pore pressure; others (McSaveney, 2002) a frictional model with space-dependent friction constant. Such models are phenomenological, i.e., the measured run-out is used to calibrate the parameters, but the physics at the rock-ice interface is not addressed.

Experiments with polite surfaces at low normal loads (Bowden, 1953; Scholz, 2002; Persson, 2000) indicate low friction force between ice and rock compared to rock against rock, and a further reduction with increasing speed and load. These observations are explained as due to the creation of a thin layer of melted water (Persson, 2000; Colbeck, 1995; Penner, 2001). However, a landslide is composed of broken blocks and it is not obvious how the irregular basal surfaces will affect the sliding against a soft, icy ground.

Studies of a hard metal sliding against a soft one have shown that the polite surface of a metal is not smooth at a microscopic scale, but presents asperities. Digging into the soft metal, the asperities of the hard metal will produce a certain number of grooves. Friction mostly results from the energy necessary to create grooves in the soft metal, an effect termed plowing (Rabinowicz, 1995). In a simple geometrical model, asperities can be modeled as cones of apex angle $\pi-2\vartheta$, where ϑ is called the roughness angle of the asperities (Rabinowicz, 1995). The friction coefficient when plowing is the dominant effect turns out to be given as $\mu_{pl} = \tan\vartheta/\pi$. For sandpaper, $\tan\vartheta \approx 0.2$ and so $\mu_{pl} < 0.1$. However, data for small rock avalanches suggest higher values (De Blasio, in preparation), which also agrees with random orientations of the blocks which would give $\tan\vartheta \approx 1$ and thus $\mu_{pl} \approx 0.3$.

It is suggested that plowing is a major source of resistance of a rock avalanche sliding on glacier, giving a velocity-independent resistance. Melt water mixed with rock debris may also contribute with a velocity-dependent resistive stress of the form $\tau \approx \eta U/\delta_W$, where η is the resulting viscosity of the slurry and δ_W is the thickness of the viscous layer, even though the effect is difficult to quantify. A similar plowing effect might also have occurred for landslides in Valles Marineris, if ice or a weak material like ice was present at the sole.

In a second scenario according to which the landslides in Valles Marineris were subaqueous, a lubrication mechanism can be suggested based on the analogy with submarine landslides on Earth. Numerous recent studies of submarine landslides have demonstrated that landslides travel with much reduced friction in water (see e.g. the data compilation in De Blasio et al., 2006). This peculiar effect, termed hydroplaning (Mohrig et al., 1998), commences when the dynamic pressure at the front of the fast-moving landslide equates the overburden pressure of the rocky material. This creates a water layer beneath the landslide sole, which strongly reduces the friction.

4. Conditions for the formation of furrows

4.1. Suggested mechanism for the creation of furrows

Having estimated the velocity of a model landslide in Valles Marineris, we can analyze the formation mechanism of furrows. Fig. 4 shows the rationale of the model suggested here. The important condition for creation of furrows is the presence of a terrain that (i) can provide a strong lubrication, as previously

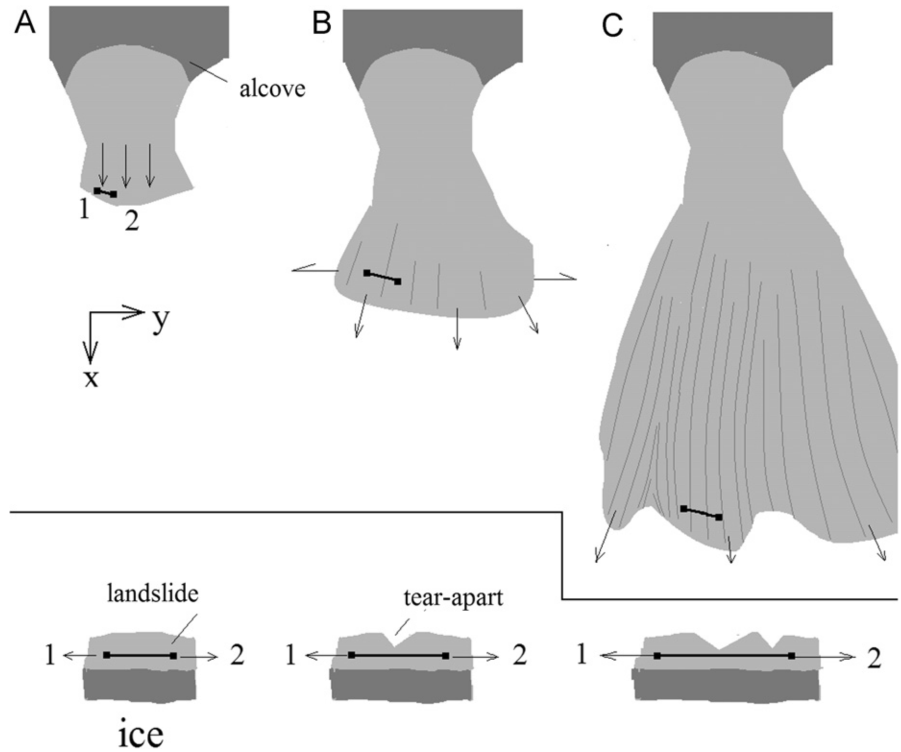

Fig. 4. Conceptual model for the formation of longitudinal furrows. A, B, and C refer to successive instants of time. The bottom panels show how furrows result from tear-apart of the granular avalanche on a soft base.

discussed, and (ii) is very soft at the base. Both conditions allow single portions of the landslide to move inertially (Dufresne and Davies, 2009) or partially following the local gradient, without much vertical disturbance.

It is suggested that furrows are created when the landslide, descending along the valley, meets a flat area and so widens in the direction perpendicular to the main flow. The lateral spreading is likely a consequence of the lateral pressure (Fig. 4). A granular heap composed of grains with internal friction coefficient μ and resting unevenly on a flat surface with basal friction coefficient $\mu_0 \ll \mu$, exerts lateral normal stresses of the form $\sigma_{xx} = -\rho g D K_{EP}(\partial D/\partial x)\cos\beta$; $\sigma_{yy} = -\rho g D K_{EP}(\partial D/\partial y)$, where K_{EP} is the earth pressure coefficient for a granular material that is stretching (the so-called active state) $K_{EP} = 2[1-[1-\cos^2\phi(1+\mu_0^2)]/\cos^2\phi]-1$, and $\phi = \tan^{-1}(\mu)$ is the friction angle of the granular material (e.g., Iverson, 1997). In the above equations, the directions x and y are taken, respectively, parallel and perpendicular to the main flow to flow, as shown in Fig. 4. With a small basal friction in the range of the friction coefficients observed for Mars ($\mu_0 < 0.2-0.4$) and using $\varphi = 35^\circ$ as a representative value for the internal friction angle, it follows $K_{EP} \approx 0.1-0.33$. Assuming a parabolic cross-section for the landslide, $z(y) = D[1-(4y^2/W^2)]$, where $z(y)$ is the top level of the landslide as a function of y, the earth-pressure force causing the granular avalanche to spread on a broader area can be calculated as

$$F_{LAT} \approx -\frac{1}{2}\rho g K_{EP}\delta L \int_0^W \frac{dz^2(y)}{dy}dy = -\frac{1}{2}\rho g K_{EP}\delta L D^2,$$

where δL is the element of landslide length along the direction x of flow. Because the mass of this slice is $\delta M \approx (2/3)\rho\delta L D W$, the lateral acceleration becomes $a \approx [(3/4)(DK_{EP}/W)]g \propto W^{-2}$, where the last equation derives from $D \propto 1/W$. The uncertainties justify the use of the initial acceleration $a \approx [(3/4)(D_0 K_{EP}/W_0)]g$ for a simple estimate instead of the full solution, where D_0, W_0 are the initial height and width of the landslide, respectively. For times of the order $\tau \approx 200$ s (approximate duration of the landslide as follows from the previous calculations), a gives the correct order of magnitude of the broadening $\Delta W \approx (1/2)at^2$ corresponding to some km to tens of km.

In short, it is suggested that as a consequence of the landslide widening, the main body was torn apart along a series of lines. The material locally adjusted its angle of dip to the angle of repose; the furrows are thus interpreted as remnants of the zone of divergence (Fig. 4).

4.2. Necessary conditions for preservation of furrows during flow

After formation, the furrows necessitate of three conditions to remain intact.

(1) The landslide should slip at the base. A velocity difference between the base and the top would generate a recirculation movement at the front, with downward velocity component (Fig. 5) that tends to obliterate the furrows. This rules out other mechanisms of enhanced mobility like rheological or Bingham fluid models for the landslide material of Valles Marineris, that are based on the premise the slippage does not occur at the base. This also substantiates the dry model for the bulk of the landslide bodies in Valles Marineris (Soukhovitskaya and Manga, 2006).

(2) A second condition concerns the basal softness. A natural terrain on which a rock avalanche travels is hard and irregularly shaped. Let us model for simplicity the terrain irregularities as a sinusoid with wave length λ (Fig. 6). The material gets sheared if the horizontal force $2\sigma_{xx}WD\mu = 2K_{EP}\sigma_{zz}WD\mu$ (where σ_{zz} is the normal stress) is much less than the weight of the material between two crests, equal to $\lambda\ W\ D\rho g$ (6 A). The criterion becomes so $\lambda W D\rho g \gg 2WK_{EP}(1/2)\rho g D^2\mu$ or simply $\chi \equiv D\mu K_{EP}/\lambda \ll 1$. Using values $\lambda = D = 10$ m, $\mu = 0.7$, it is found $\chi \approx 0.2$. This indicates that the rock avalanche will likely fail along shear zones, as shown in Fig. 6B, and furrows will be significantly disturbed in the long run (Fig. 6C). In contrast, in

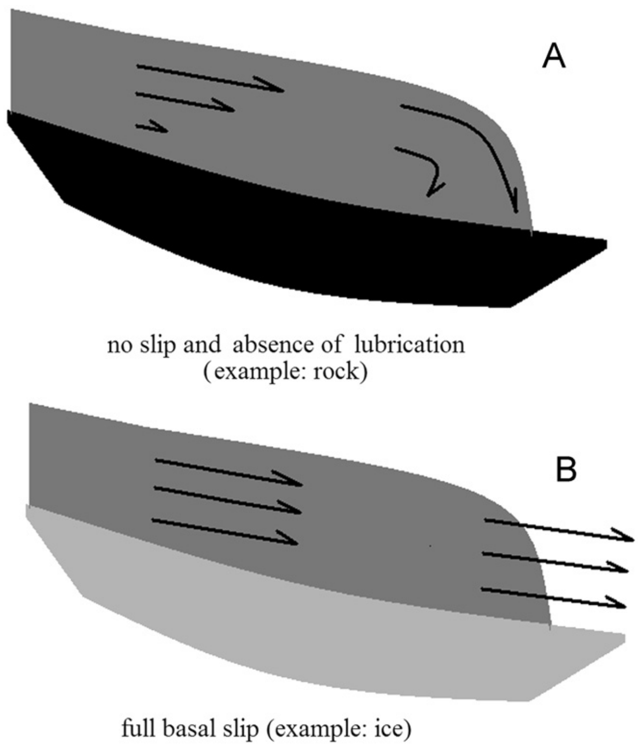

Fig. 5. Absence of slip at the base like in (A) implies a circular movement at the front similar to a conveyor belt. This kinematics destroys the furrows. In the presence of basal lubrication, the landslide moves parallel to the ground (B).

the presence of a soft terrain the landslide will cut into the ground, damping out vertical movements (Fig. 6D and E).

(3) A landslide traveling in a viscous medium like air or water is subjected to skin friction shear stress $\approx (1/2)\rho_A C_{SF} U^2$ that tends to displace the blocks on the top. For furrows to be preserved, this stress must be much less than the erosion threshold, which leads to the condition (e.g., Robert, 2003): $(1/2)\rho_F C_S U^2 \leqslant 0.05(\rho-\rho_F)gd$, where d is the characteristic block diameter. After minor manipulation the condition becomes

$$r \equiv \frac{10\rho_F}{\rho-\rho_F} C_S \frac{U^2}{\text{gd}} \ll 1. \qquad (2)$$

For Sherman, values $r \approx 0.03-0.05$ can be estimated with $d=50$ cm (Shreve, 1966) and a velocity of 40 m/s, so that condition (2) is also satisfied for blocks of only few cm in diameter. This explains the presence of small blocks on the surface of the Sherman landslide. Yet smaller values for the ratio r are obtained for a subaerial landslide on Mars. However, based on the calculated subaqueous velocities shown in Fig. 1, much greater values ($r \approx 50-80$) are found in the hypothesis that the landslides in Valles Marineris were subaqueous with a maximum velocity of 59 m/s (Fig. 3). The high values for the shear stress result from the greater density of the medium, which entails strong erosion on top of the moving landslide. This indicates that furrows would not have been conserved in a subaqueous environment at the calculated speeds (and furrows are indeed uncommon on the top of subaqueous landslides on Earth, Dufresne and Davies, 2009).

Another criterion can be applied to test whether the landslides of Valles Marineris were subaqueous or subaerial. Experiments (Ilstad et al., 2004) and real in situ underwater observations (De Blasio, 2011) show that the front of subaqueous debris flows is subject to an intense force that may make it "flip" backward. Let us consider a simple model of the front as a slab joint at the base and subjected to a drag stress directed backward (Fig. 7). The

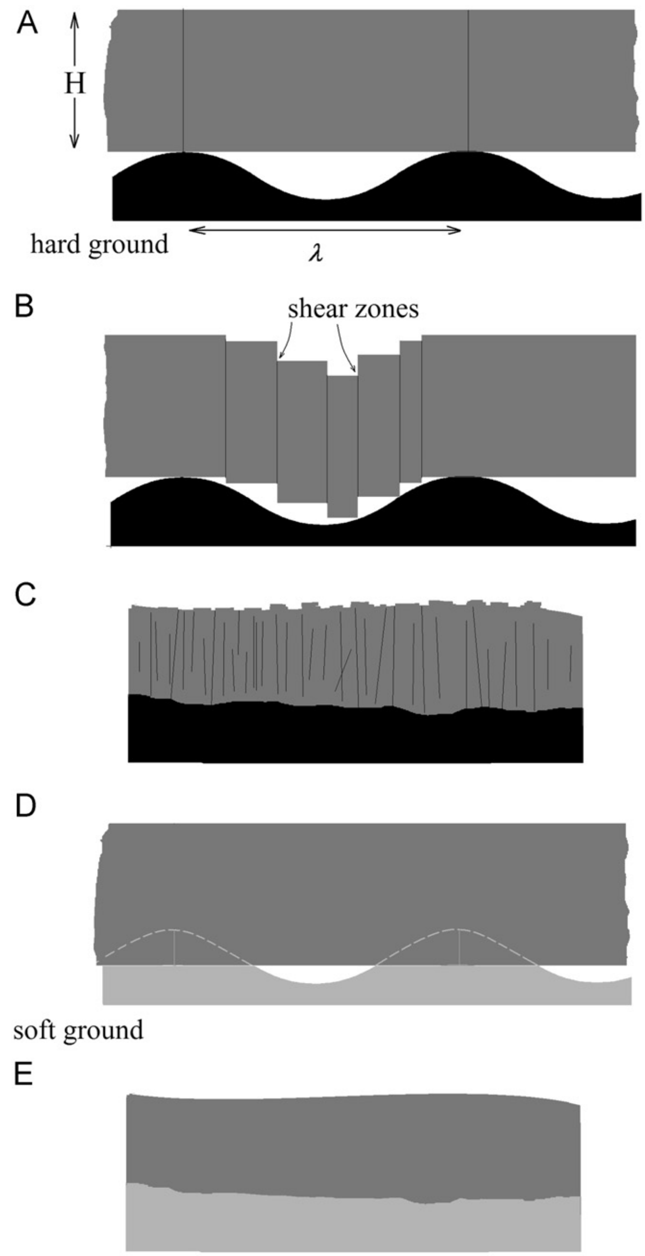

Fig. 6. Formation of vertical shear zones. A: the landslide is sheared due to the irregularities of the ground (here modeled as a sinusoidal disturbance) with whatever orientation and collapses (B) along shear zones, so disturbing the top (C). On a soft ground the avalanche cuts into the base (D) reducing the vertical disturbance to a minimum (E).

equation for the angular acceleration of the front is found as

$$\ddot{\theta} = \frac{-T\Delta\rho g\cos\theta + (1/2)\rho_F C_D \sin^2\theta U^2}{(2/3)lT\rho}, \qquad (3)$$

where T and l are the slab thickness and length, respectively, and θ is the angle of the slab from the horizontal direction (Fig. 7). In order to reach a positive value of $\ddot{\theta}$, the slab must start from a minimum angle, as $\theta=0$ is evidently an equilibrium point. As observed in the experiments (Ilstad et al., 2004), the increase in the angle of attack may result from the lift force on top of the debris flow, similar to the one acting on airfoils. From Eq. (3), it follows that for a given initial attack angle, a positive value for $\ddot{\theta}$ (and thus front flipping) is determined by the dimensionless

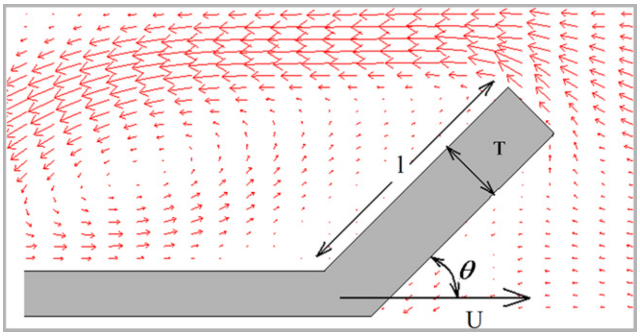

Fig. 7. Flipping flont of a landslide moving in water.

number flipping number

$$Fl = \frac{U^2}{gT}\frac{\rho_F}{\Delta\rho}C_D. \quad (4)$$

In the experiments of Ilstad et al. (2004), where the debris flow was often observed to flip, Fl was about 1. Based on the calculated values of the velocity (Fig. 2), the estimate for the Martian slides is $4 \leq Fl \leq 7$. It can be inferred that if the Valles Marineris landslides had been subaqueous, a flipped front would have resulted for at least some deposits (and probably for most of them), whilst the examination of the images shows otherwise.

4.3. Further remarks

It is important to point out that not all landslides traveling on glaciers exhibit neat furrows. Even restricting ourselves to landslides belonging to the same landslide Alaskan swarm, we can note that the Allen avalanche 4 was thick and bulky, whereas the Allen Glacier avalanche developed digitations presumably due to running blocks or internal shearing, rather than furrows (Post, 1968; Johnson and Ragle, 1968). Thus, the phenomenology of landslides falling on glaciers is certainly more variegated, Sherman representing only one kind of typology. Moreover, there are examples of landslides that were likely lubricated at the base by a medium other than ice, and did not develop apparent furrows. The best example is probably the Blackhawk landslide, probably lubricated by a thin water layer (Erismann and Abele, 2001).

A final useful observation concerns the increase in the curvature of the furrows as a function of the distance from the headwall, discernible in many of the Valles Marineris landslides. In Fig. 2, the terminus of a landslide in Ganges Chasma is used as an example showing clearly curved furrows in the zone "D" of the figure. Consider the landslide material moving along a certain length with speed U_x along x, where a reference system as in Fig. 4 is adopted with x pointing toward the main flow direction. We assume a slope gradient with angle γ along y representing a local topographic disturbance. A simple kinematic analysis in which friction is neglected shows that the material trajectory follows a path described by the following equation:

$$\frac{dy}{dx} \approx \frac{\sqrt{2g\sin\gamma y}}{U_x}; \quad y = \frac{g\sin\gamma}{2U_x^2}x^2. \quad (5)$$

These equations show that the trajectory is bent with a curvature that decreases with the translational velocity. In the zone C of Fig. 2 the landslide velocity U_x was high, as shown in Fig. 3. In this situation, the denominators of Eq. (5) become large, which implies $dy/dx \approx 0$, i.e., trajectory and furrows remain straight. However, as the landslide decreased speed, the curvature of the trajectory became noticeable, as the denominators of Eq. (5) decreased in magnitude. Thus, depending on the local topography expressed by the angle γ, the landslides may exhibit a terminal bending of the front, as well visible in the zone D of the example of Fig. 2. This shows once more that the mass flows in Valles Marineris have been fast-moving landslides.

5. Conclusions

Based on analogy with the glacial landslide on Earth and on the calculations presented, the most natural conclusion is that the landslides of Valles Marineris (i) were lubricated at the base, and (ii) the terrain was soft. There are four most likely possibilities for the nature of the basal medium.

5.1. Ice

Ice as lubricating medium has been suggested earlier in this paper in analogy with terrestrial examples. A problem with ice is that because the landslides in Valles Marineris exhibit very different ages (Quantin et al., 2004), the model requires the endurance of ice in Valles Marineris throughout billions of years. It is unlikely that ice remained exposed for very long time because at the present atmospheric pressure it would promptly sublimate at the low latitude of Valles Marineris. Neither could a flowing glacier reside in Valles Marineris in similitude with the Sherman glacier, as the flowage of ice would displace the landslide deposits in a geologically instantaneous time. One possibility is that because the climate of Mars changed considerably in the past due to chaotic change of Mars obliquity (Laskar et al., 2004), perhaps during some periods Valles Marineris was sufficiently cold and ice could be formed at the valley bottom. However, even in this case it is difficult to explain why landslide activity occurred only during these periods. Although there seems to exist a relationship between glaciation–deglaciation cycles and slope instability on Earth (von Porchinger, 2002), it is unlikely that no failures occurred in periods of more temperate climate.

Another possibility is that ice was subsurface, as long-life permafrost is more likely to persist from middle latitudes (e.g., Clifford and Hillel, 1983; Kargel, 2004). The thickness eroded by a landslide sliding on a soft surface can be estimated as

$$\frac{d\delta}{\mathrm{d}t} \approx \frac{\rho g D\cos\beta}{p}\frac{\tan\vartheta}{\pi}U, \quad (6)$$

where ϑ is the already defined roughness angle of the asperities and p is the penetration hardness (see e.g., Rabinowicz, 1995), which for pure ice depends on the temperature; indicatively, $p \approx 4-8$ MPa (Bowden, 1953). Higher values are probably better suited for sub-surface ice, because debris certainly adds strength to the ice layer. Erosion rates of some millimeters to some centimeters per second are obtained from Eq. (6) for pure ice, for a total erosion depth of $\delta \approx \rho gHR\cos\beta\tan\vartheta/(p\pi)$, where R is the run-out. This amounts to a maximum of 10 m for pure exposed ice, and perhaps something less for sub-surface ice, to a degree that is difficult to ascertain. These tentative estimates indicate that the landslides in Valles Marineris could have in principle excavated a superficial protective debris-ice layer, exposing soft subsurface ice. It is not clear whether glacial conditions and permafrost were attained in the Valles Marineris during some period of Mars history. Whereas most climatological studies admit enduring frosty climate only far from equatorial areas, and Shallow Radar (SHARAD) observations report presence of debris-covered ice only at higher latitudes (Holt et al., 2008), there are also indirect geochemical indications of glacial conditions at equatorial regions (Niles and Michalski, 2009).

5.2. Deep water (e.g., lakes)

The possible presence of lakes in Valles Marineris and other locations has been suggested based on sedimentological and morphological considerations (see e.g. Lucchitta, 2009 and references therein; Metz et al., 2009). Although the temporary presence of lakes in Valles Marineris is well possible, the present analysis tends to exclude subaqueous emplacement of the landslides.

5.3. Shallow water layer

While the above dynamical analysis indicates as unlikely that the landslides in Valles Marineris were completely submerged, lubrication by shallow water layers, for example in the form of ponds not completely embedding the landslide, is not completely ruled out by the present calculations, because the critical condition (3) for the preservation of furrows applies only if the upper surface of the landslide is covered by water. Landslides falling on shallows coasts, geometrically similar to the landslides of Valles Marineris, often show long runout (Hutchinson, 2002) probably due to vigorous dilution and sediment liquefaction (Hutchinson, 2002) or efficient lubrication by the shallow water (De Blasio, 2011), but not longitudinal striations. Unfortunately, no dynamical models are available to treat the dynamics of these particular landslides. However, the fact that coastal landslides do not exhibit furrows points to a high degree of disturbance of the landslide material and is indication against this kind of lubrication mechanism.

5.4. Evaporites

The presence of sedimentary rocks in Valles Marineris and other locations on Mars, suspected for the first time during the Mariner 9 mission, is now well established. Of particular interest for the present topic is the presence of beds of evaporites in Meridiani Plenum, Juventae Chasma or Chandor Chasma, probably deriving from water evaporation subsequent to early wet period (see e.g. Metz et al., 2009; Ross Taylor and McLennan, 2009; Wezel and Baioni, 2010). Sulphate beds like gypsum or anhydrite, other potassium or calcium-rich salts, clays or oxides may confer a soft layer with lower friction coefficient than the basaltic rocks assumed for Valles Marineris, and would likely result in sliding dynamics similar to ice. For example, the point load strength of anhydrite and gypsum are of the order 1–5 and 0.2–2.4 MPa, respectively, less than that of basalt, which is about 16.9 MPa (Bell, 2007). Perhaps the sliding of hard rock on evaporites can be explained with a plowing mechanism similar to the rock on ice discussed in Section 3, which would also entail a lower friction coefficient on rock. The presence of weak layers of evaporites would also explain the pervasive failures in Valles Marineris without the need for water pore pressure in the sediments or marsquakes requiring accelerations of the order 0.2 g (Bigot-Cormier and Montgomery, 2007). Because examples of landsliding on evaporite beds are hard to find on the Earth, numerical modeling will probably represent a viable alternative for the investigation of the dynamics of landslides on evaporite beds.

To conclude, the dynamics of landslides in Valles Marineris is a complicated issue involving the mechanics of rocky materials, rheology, and fluid mechanics. There is no doubt that a better understanding of landslide dynamics on Mars will shed like on the mysteries of Mars climatology.

Acknowledgements

Two anonymous reviewers considerably improved the quality of the paper. In particular, one of the reviewers pointed out the large diversity of landslides structures when falling on glaciers, while the second referee suggested evaporites as possible lubricating layers during the failure of the Valles Marineris landslides.

References

Adushkin, V.V., 2006. Mobility of Rock avalanches triggered by underground nuclear explosions. In: Evans, S.G., Scarascia Mugnozza, G., Strom, A., Hermanns, R. (Eds.), Landslides from Massive Rock Slope Failure,NATO Science Sereis. Springer.

Bell, F.G., 2007. Engineering Geology. Elsevier, Amsterdam.

Bigot-Cormier, F., Montgomery, D.R., 2007. Valles Marineris landslides: Evidence for a strength limit to Martian relief? Earth and Planet. Sci. Lett. 260, 179–186.

Bowden, F.P., 1953. Friction on snow and ice. Proc. R. Soc. (London) A 217, 462–478.

Carr, M., Head III, J.W., 2003. Oceans on Mars: as assessment of the observational evidence and possible fate. J. Geophys. Res. 108, 5042.

Carr, M., 2006. The Surface of Mars. Cambridge University Press, Cambridge.

Clifford, S.M., Hillel, D., 1983. The stability of ground ice in the equatorial region of Mars. J. Geophys. Res. 88, 2456–2474.

Colbeck, S.C., 1995. Pressure melting and ice skating. Am. J. Phys. 63, 888–890.

Crosta, G.B., Frattini, P., Fusi, N., 2007. Fragmentation in the Val Pola rock avalanche, Italian Alps. J. Geophys. Res. 112. doi:10.1029/2005JF000455.

Davies, T.R.H., McSaveney, M.J., 1999. Runout of dry granular avalanches. Can. Geotech. J. 36, 313–320.

De Blasio, F.V., Elverhøi, A., Engvik, L.E., Issler, D., Gauer, P., Harbitz, C., 2006. Understanding the high mobility of subaqueous debris flows. Norw. J. Geol. 86, 275–284.

De Blasio, F.V., 2009. Rheology of a wet, fragmenting granular flows and the riddle of the anomalous friction of large rock avalanches. Gran. Matter 11, 179–184.

De Blasio, F.V. The aureole of Olympus Mons (Mars) as the compound deposit of submarine landslides. Earth and Planetary Science Letters, submitted for publication.

De Blasio, F.V., 2011. Physical Introduction to Landslides. Springer Verlag, Berlin.

Erismann, T.H., Abele, G., 2001. Dynamics of Rockslides and Rockfalls. Springer, Berlin.

Dufresne, A., Davies, T.R., 2009. Longitudinal ridges in mass movement deposits. Geomorphology 105, 171–181.

Ilstad, T., De Blasio, F.V., Elverhøi, A., Harbitz, C.B., Engvik, L., Longva, O., Marr, J., 2004. On the frontal dynamics and morphology of submarine debris flows. Marine Geol. 213, 481–497.

Harrison, K.P., Grimm, R.E., 2003. Rheological constrains on martial landslides. Icarus 163, 347–362.

Harrison, K., 2010. Private communication.

Holt, J.W., Safaeinili, A., Plaut, J.J., Head, J.W., Phillips, R.J., Seu, R., Kempf, S.D., Choudhari, P., Young, D.A., Putzig, N.E., Biccari, D., Gim, Y., 2008. Radar sounding evidence for buried glaciers in the southern mid-latitudes of Mars. Science 322, 1235–1238. doi:10.1126/science.1164246.

Hutchinson, J.N., 2002. Chalk flows from the coastal cliffs of northern Europe, in: Evans, S.G. and DeGraaf, J.V. (Eds.), Catastrophic landslides: Effects, Occurrence, and Mechanisms, Geol. Soc. Am. Rev. Eng. Geol., vol. 55.

Hsü, K.J., 1975. Catastrophic debris streams (Sturzstroms) generated by rockfalls. Geological Society of America Bulletin 86, 129–140.

Iverson, R., 1997. The physics of debris flows. Reviews of Geophysics 35, 245–269.

Johnson, N.M., and Ragle, R.H. 1968. Analysis and Flow Characteristics of Allen II Slide from Aerial Photographs. In: The Great Alaska Earthquake of 1964. Vol. 3: Hydrology, part A. Commettee on the Alaska Earthquake of the division of Earth Science, National Academy of Sciences, Washington, USA, 369–373.

Kargel, J.S., 2004. Mars: A warmer, wetter Planet. Springer Praxis, London.

Legros, F., 2002. The mobility of long-runout landslides. Engineering Geology 63, 301–331.

Laskar, G., Gastineau, M., Joutel, F., Levrard, P., Correia, A., 2004. Long term evolution and chaotic diffusion on the insulation quantities of Mars. Icarus 170, 264–343.

Lajeunesse, E., Mangeney-Castelnau, C., Vilotte, J.P., 2006a. Spreading of a granular mass on a horizontal plane. Phys. Fluids 16, 2371–2381.

Lajeunesse, E., Quantin, C., Allemand, P., Delacourt, C., 2006b. New Insight on the runout of large landslides in the Valles-Marineris Canyons, Mars. Geophysical Research Letters L04403, 33.

Locat, P., Couture, R., Leroueil, S., Locat, J., Jaboyedoff, M., 2006. Fragmentation energy in rock avalanches. Can. Geotech. J. 43, 830–851.

Lucchitta, B.K., 1979. Landslides in Vallis Marineris, Mars. J. Geoph. Res 84, 8097–8113.

Lucchitta, B.K., 2009. Lakes in Valles Marineris, Mars (II): valleys, channels, shallow lakes, and age. 40th Lunar and Planetary conference.

Marangunic, C., and Bull, C. 1968. The landslide on the Sherman Glacier. In: The Great Alaska Earthquake of 1964. Vol. 3: Hydrology, part A. Commettee on the

Alaska Earthquake of the division of Earth Science, National Academy of Sciences, Washington, USA, 383–394.
McSaveney, M., 1978. Sherman glacier rock avalanche, Alaska, U.S.A. In: Voight, B. (Ed.), Rockslides and avalanches. Elsevier, Amsterdam, The Netherlands.
McSaveney, M. 2002. Recent rockfalls and rock avalanches in Mount Cook National Park, New Zealand. in: *Catastrophic Landslides: Effects, Occurrence, and Mechanisms*. S.G. Evans e J.V. DeGraff (a cura di). The Geological Society of America, Boulder.
Metz, J.M., Grotzinger, J.P., Mohrig, D., Milliken, R.E., Prather, B., Pirmez, C., McEwen, A.S., Weitz, C.M., 2009. Sublacustrine depositional fans in southwest Melas Chasma. Journal of Geophysical Research 114, E10002.
Mohrig, D., Whipple, K.X., Hondzo, M., Ellis, C., Parker, G., 1998. Hydroplaning of subaqueous debris flows. Geol. Soc. Am. Bull 110, 387–394.
Niles, P.B., Michalski, J., 2009. Meridiani Planum sediments on Mars formed through weathering in massive ice deposita. Nature Geoscience 2, 215–220.
Parker, T.J., Gorsline, D.S., Saunders, R.S., Pieri, D., Schneeberger, D.M., 1993. Coastal Geomorphology of the Martian northern plains. J. Geophys. Res. 98, 11,061–11,078.
Penner, A.R., 2001. The physics of sliding cylinders and curling rocks. Am. J. Phys 69, 332–339.
Persson, B.N.J., 2000. Sliding friction. Physical principles and applications. Springer Verlag, Berlin.
Rabinowicz, E., 1995. Friction and wear of materials. Wiley-Interscience, New York.
Post, A.S. 1968. Effects on glaciers. In: The Great Alaska Earthquake of 1964. Vol. 3: Hydrology, part A. Commettee on the Alaska Earthquake of the division of Earth Science, National Academy of Sciences, Washington, USA, 266–308.
Robert, A., 2003. River Processes. Arnold, London.
Ross Taylor, S., McLennan, S.M., 2009. Planetary crusts: their composition, origin and evolution. Cambridge University Press, Cambridge.
Scheidegger, A.E., 1973. On the prediction of the release and velocity of catastrophic rockfalls. Rock Mechanics 5, 231–236.
Schulz, R.A., 2002. Stability of rock slopes in Valles Marineris, Mars. Geophys. Res. Lett., 29. doi:10.1029/2002GL015728.
Schlichting, H., 1960. Boundary layer theory. McGraw-Hill, New York.
Scholz, C.H., 2002. The mechanics of Earthquakes and Faulting, 2^{nd} ed. Cambridge University Press, Cambridge.
Shea, T., van Wyk de Vries, B., 2008. Structural analysis and analogue modeling of the kinematics and dynamics of rockslide avalanches. Geosphere 4, 657–686.
Shreve, R.L., 1966. Sherman landslide. Alaska: Science 154, 1639–1643.
Sreve, R.L. 1968.Sherman Landslide. In: The Great Alaska Earthquake of 1964. Vol. 3: Hydrology, part A. Commettee on the Alaska Earthquake of the division of Earth Science, National Academy of Sciences, Washington, USA, 395–401.
Sosio, R., Crosta, G.B., Hungr, O., 2008. Complete dynamic modeling calibration for the Thurwieser rock avalanche (Italian Central Alps). Engin. Geol 100, 11–26.
Soukhovitskaya, V., Manga, M., 2006. Martian landslides in Valles Marineris: Wet or dry? Icarus 180, 348–352.
Quantin, C., Allemand, P., Mangold, N., Delacourt, C., 2004. Ages of Valles Marineris (Mars) landslides and implications for canyon history. Icarus 172, 555–572.
Von Porchinger, A. 2002. Large rockslides in the Alps: A commentary on the contribution of G. Abele (1937-1994) and a review of some recent developments. In *Catastrophic Landslides*, Evans S.G. e DeGraff, J.V. (a cura di). Geol. Soc. Am. Rev. Eng. Geol. Vol. XV.
Wezel, F.C., Baioni, D., 2010. Evidence for subaqueously resedimented sulphate evaporites on Mars. Planetary and Space Science 58, 1500–1505.